

# EFFECTS OF DRYING CONDITIONS ON POLYVINYL ALCOHOL–WATER AND CELLULOSE ACETATE–TETRAHYDROFURAN FILMS

IONUT OVIDIU FORȚU,\* CIPRIAN NEGOESCU\*\* and IOAN MĂMĂLIGĂ\*

\**Department of Chemical Engineering, “Gheorghe Asachi” Technical University of Iasi, 73, Prof. Dr. Docent Dimitrie Mangeron Str., 700050, Iasi, Romania*

\*\**School of Chemical Engineering, University of Birmingham, Edgbaston B15 2TT, Birmingham, United Kingdom*

✉ *Corresponding author: Mamaliga Ioan, imamalig@tuiasi.ro*

*Received January 7, 2019*

Polymer films and membranes play an important role in modern industries that use paints and varnishes, magnetic tapes, CDs, adhesives, foil stickers, pharmaceutical patches, solar cells, wastewater treatment *etc.* The properties of these films and membranes depend strongly on the drying conditions, including thermodynamic equilibrium, diffusion coefficients, thermal agent temperature and velocity. This paper presents the effects of temperature and air velocity on the drying of polyvinyl alcohol and cellulose acetate films.

The drying studies were carried out on two systems: polyvinyl alcohol–water and cellulose acetate–tetrahydrofuran, aiming to highlight the influence of temperature and velocity of the drying gas on the polymer films. Unlike the polyvinyl alcohol films, which, after drying, have a compact structure, the cellulose acetate films have a porous structure, with pores of approximately 1 micrometer diameter.<sup>1</sup> This difference in structure was also evidenced by the different profiles of the drying curves of the solutions obtained by dissolving the two polymers in water and tetrahydrofuran, respectively.

**Keywords:** polyvinyl alcohol, cellulose acetate, films, drying behavior

## INTRODUCTION

Removing volatile solvents from a polymer film is a complicated process, because it involves simultaneous mass and heat transfer. This process is also controlled by complex transport mechanisms and the thermodynamic behavior of polymer solutions. The structure and properties of polymer films are greatly influenced by the way drying occurs. The theoretical description of drying is greatly complicated by the vapor–liquid balance from the polymer film interface and the drying gas, diffusion coefficients that strongly depend on temperature and concentration, and the state of the polymer.<sup>2</sup>

As most coatings are obtained by evaporating the solvent from a dilute initial solution, understanding the kinetics of drying polymer solutions is a major problem in many industrial processes.<sup>3</sup> The kinetics of drying generally reveals two steps. In the first rapid step, the solution is still rather dilute and the solvent concentration is high enough to allow an important flux to the interface. The evaporation flux is similar to that obtained by the evaporation of a pure solvent. In this fast step, the kinetics depends on the heat and mass transfer between the interface and the gas. In the second step, the solvent concentration declines, diffusion decreases significantly, and the properties of the solution have an important influence on this slow period.

Drying of polymeric films requires the removal of the solvent, which is carried out in specialized installations and depends on the temperature, the properties of the gaseous phase, the flow regime, the dryer geometry *etc.*

Huang *et al.*<sup>4</sup> have developed an experimental method for determining the sorption kinetic curves of two solvent mixtures (ethanol/1,2 dichloroethane and ethanol/ethyl acetate) in polyurethane and proposed a transport model for the sorption of solvent mixtures in polymer membranes. Good consistency of the experimental data with those reported in the literature was found, and because the model parameters are independent of the solvent mixture composition, the model has the ability to estimate the transport phenomena of solvent mixtures in polymeric membranes. The transfer of the solvent in the second step involves several complex phenomena, including the reduction of the solvent/polymer diffusion coefficient by several orders of magnitude when the concentration of

solvent is decreased.<sup>5</sup> Because of limitations imposed by environmental regulations, the use of volatile organic solvents is reduced in favor of aqueous solutions.

With virtually non-existent toxicity and good water solubility, polyvinyl alcohol presents an increased interest for application in various fields, including the pharmaceutical industry, food, biosensors and combustion cells.<sup>6</sup> Transport properties in cellulose acetate films have been investigated by many researchers, due to the wide applications of these films and membranes in pharmacology,<sup>7</sup> wastewater treatment,<sup>8,9</sup> tissue engineering<sup>10</sup> *etc.* Diffusion processes in cellulose acetate films depend on the degree of acetyl substitution, film thickness, structure<sup>11</sup> *etc.*

The main objective of the research reported in this paper is the study of the influence of the main factors contributing to the drying of polymer films. In the experiments, two polymer-solvent systems will be investigated: polyvinyl alcohol-water (PVA-W) and cellulose acetate-tetrahydrofuran (CA-THF).

## EXPERIMENTAL

### Materials

Drying studies were carried out on solutions and thin films of the polymers shown in Figure 1.

### Polymer properties

Polyvinyl alcohol (PVA) can be obtained by hydrolyzing polyvinyl acetate. PVA is a synthetic, linear, non-toxic semi-crystalline polymer, biocompatible, biodegradable and water-soluble at temperatures above its glass transition (85 °C).<sup>12</sup> The water solubility and physical properties of PVA, including its film form, are highly affected by the degree of hydrolysis, molecular weight and its crystal precipitation.<sup>13</sup> A PVA-water film was prepared as follows: to prepare a 5% solution of PVA in water, 5 mg of PVA powder (from Merck, with an average molecular weight of 89000-98000, d = hydrolysis degree of 98%) was dissolved in 95 mL of double-distilled water.

Cellulose acetate (CA) is the most important cellulose ester due to its low cost, non-toxicity, biodegradability and renewable source. CA is obtained by the reaction of cellulose with acetic anhydride and acetic acid, using sulfuric acid as a catalyst.<sup>14</sup> The reaction is composed of a two-stage acetylation process and it is followed by a hydrolysis reaction, so that we can obtain CA with a 2.45-2.5 degree of substitution. The polymer has an acetate group on approximately 2.45-2.5 of every three hydroxyls.<sup>15</sup> CA powder from Merck, with an average molecular weight of ~30000, 3% max. water impurities and 1.3 g/mL density at 25 °C, was used.

### Solvent properties

The solvents used to solubilize the polymers were tetrahydrofuran (THF) and water (W). THF is a cyclic ether and a highly volatile organic solvent used in several applications.<sup>16</sup> The solvent was obtained from Chemical Company, having 72.11 g/mol molecular weight and 0.89 g/mL density.

### Experimental equipment

The drying studies of the polymeric films were carried out on the polyvinyl alcohol (PVA)-water and cellulose acetate (CA)-tetrahydrofuran (THF) systems. Unlike the PVA films, which exhibit a compact structure after drying, the CA films have a porous structure.<sup>1</sup> This structural difference will also be highlighted by the different profile of their drying curve.

The drying studies of polymeric films were carried out on a laboratory plant, schematically presented in Figure 2.

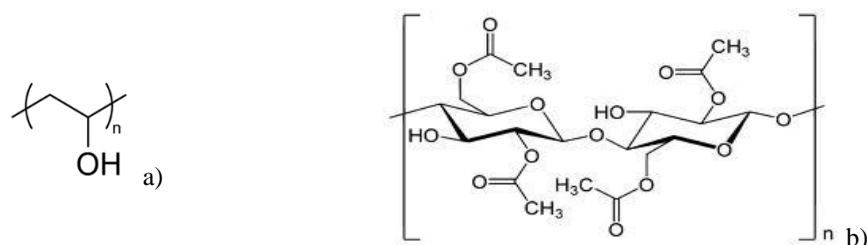


Figure 1: Chemical structure of a) polyvinyl alcohol (PVA) and b) cellulose acetate (CA)

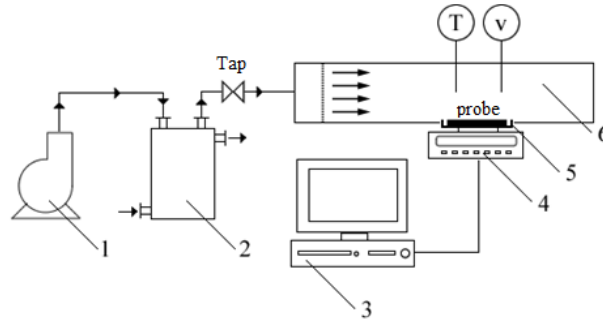


Figure 2: Laboratory set-up used for polymer drying studies

The experimental laboratory set-up was composed of a fan (1), a heat exchanger (2), a tap, a computer (3), an analytical balance (0.1 mg precision) (4), a probe tray (5), a drying tunnel (6), a temperature sensor (T) and an anemometer (v). The drying gas given by the medium pressure fan (1) goes through the heat exchanger (2) and reaches the drying tunnel (6), where the probe is situated. The velocity of the drying gas is controlled using the tap, while the temperature and velocity are measured using the temperature sensor (T) and the anemometer (v). The temperature of the drying gas was maintained constant using a Julabo F12 thermostat.

## RESULTS AND DISCUSSION

### Gas velocity influence

#### *Polyvinyl alcohol-water system*

In order to highlight the influence of the drying gas velocity, experiments on the PVA-water system were performed at 0.2, 0.4 and 0.8 m/s at four temperature values: 40, 45, 50 and 60 °C, with a 5% mass concentration of the initial polymer solution.

The normalized mass is calculated as the ratio between the solution mass at time  $t$  and the initial mass of the solution:  $t_0$ :  $m(-) = m_t/m_{t_0}$ .

Each drying curve contains three areas, as described below.

**Area 1** starts at the beginning of the experiment, where we can notice a pronounced linear decrease of the  $m(-)$  value in time. The drying kinetics is controlled by gas velocity and rapid solvent evaporation is due to a high diffusion coefficient.

**Area 2** follows the first area and the drying kinetics is controlled by gas velocity and by solvent diffusion.

**Area 3** represents the last drying stage, where we can notice a negligible influence of gas velocity. The  $m(-)$  variation presents a linear decrease and the drying kinetics is controlled by the small value of the diffusion coefficient in the almost dried film.

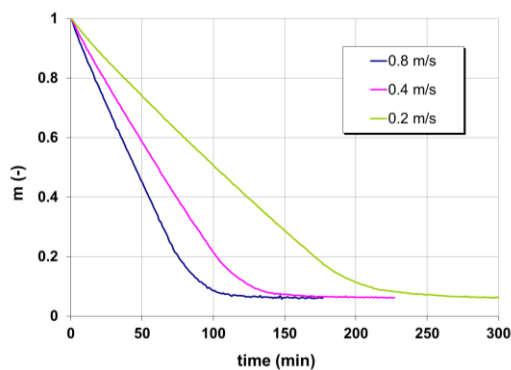


Figure 3: Drying curve of PVA-water at 40 °C gas temperature

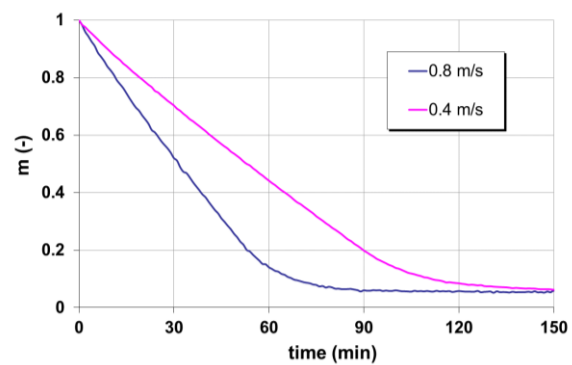


Figure 4: Drying curve of PVA-water at 45 °C gas temperature

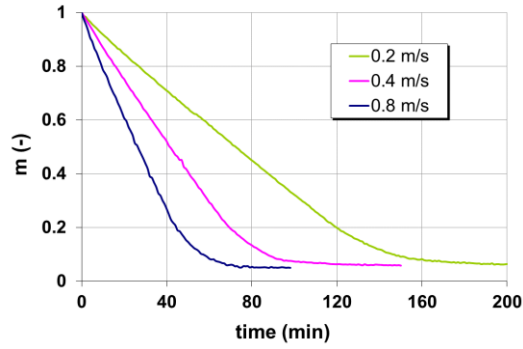


Figure 5: Drying curve of PVA-water at 50 °C gas temperature

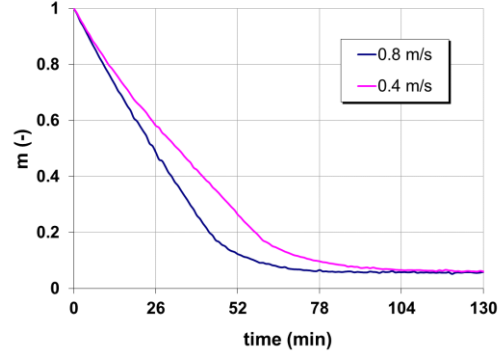


Figure 6: Drying curve of PVA-water at 60 °C gas temperature

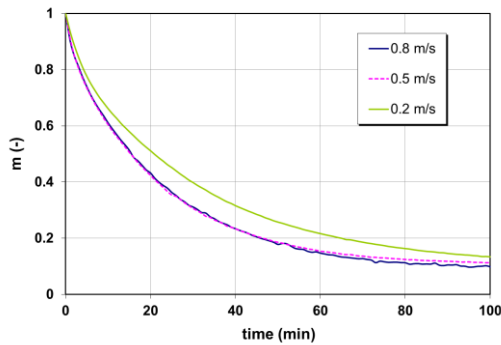


Figure 7: Drying curve of CA-THF at 30 °C gas temperature

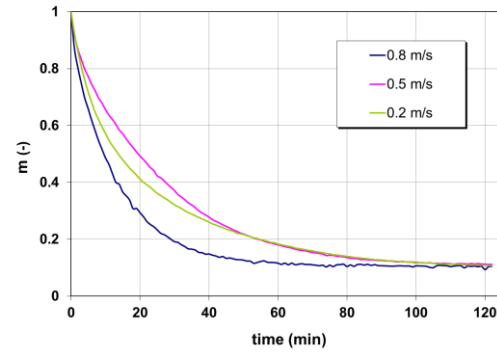


Figure 8: Drying curve of CA-THF at 40 °C gas temperature

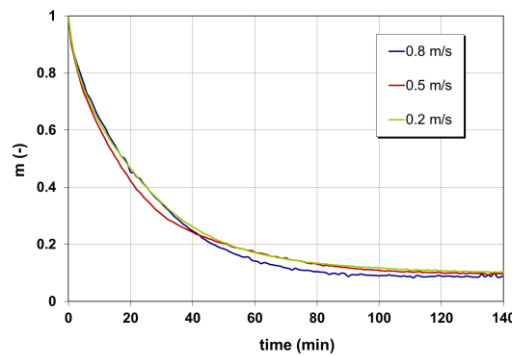


Figure 9: Drying curve of CA-THF at 50 °C gas temperature

At temperatures of 45 °C and 60 °C, the drying behavior of the PVA-water system was investigated at two values of the drying gas (0.4 and 0.8 m/s), because at lower temperature, the 0.2 m/s velocity has an insignificant influence (Figs. 4 and 6).

### ***Cellulose acetate-tetrahydrofuran***

Experiments were carried out at 30, 40 and 50 °C for three velocities of the drying gas: 0.2, 0.5 and 0.8 m/s. The drying curve is different from the previous one, in the sense that the three drying zones cannot be clearly indicated.

From the figures showing the drying curves, one can see an area corresponding to a large amount of solvent in the sample, where the normalized mass varies non-linearly with time and continues with a zone characterized by small solvent content, where  $m(-)$  decreases linearly with time. The drying curves intersect at certain points and even overlap in certain areas, which reveals a complex behavior when removing the solvent.

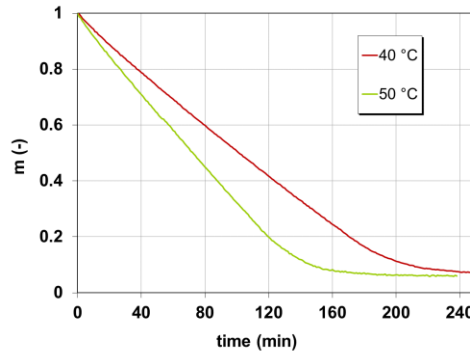


Figure 10: Drying curve of PVA-water at 0.2 m/s gas velocity

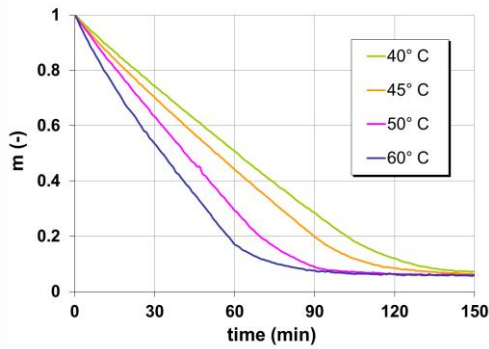


Figure 11: Drying curve of PVA-water at 0.4 m/s gas velocity

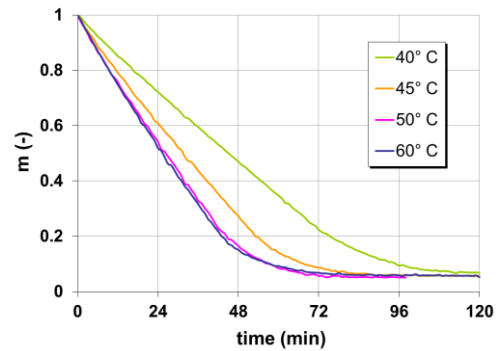


Figure 12: Drying curve of PVA-water at 0.8 m/s gas velocity

### Temperature influence

#### *Polyvinyl alcohol-water system*

In order to show the influence of temperature on the drying process, the variation of the normalized mass over time is plotted at the same gas velocity, but at different temperatures. Figures 11 and 12 show a positive influence on the drying time up to the second zone inclusive, after which the kinetics is no longer influenced by gas velocity.

At the gas velocity of 0.8 m/s, the kinetic curves are identical over the time interval investigated at temperatures of 50 and 60 °C. This indicates the possibility of skin appearance on the surface of the solution, and the process is controlled by the diffusion coefficient of the solvent through this skin, which is smaller by an order of magnitude than the diffusion coefficient in the solution (Fig. 12).

#### *Cellulose acetate-tetrahydrofuran*

For the CA-THF system, temperature does not have a significant influence on the drying process, as we can see from Figures 13, 14 and 15. An exception is the drying curve at 40 °C gas temperature and 0.8 m/s gas velocity. The drying curves for the 0.2 and 0.5 m/s gas velocity and different temperatures show clearly the negligible influence of gas temperature.

Analyzing the shape of the curves in Figures 13, 14 and 15, we can notice that the influence of the drying temperature does not seem to have a major contribution, as in the case of the PVA-water systems, unless the drying was carried out at 40 °C and a gas velocity of 0.8 m/s (Fig. 15). This drying behavior of the CA-THF system can be caused by the porous structure of the polymer film obtained. According to the literature,<sup>1</sup> drying this type of solution leads to the formation of films with pore sizes of about 1 micrometer.

### Modeling of polymer film drying

The physical model considers a polymer film disposed on a flat surface of initial thickness  $\delta = \delta_0$  at  $t = 0$  and the temperature is considered uniform ( $T_0$ ).

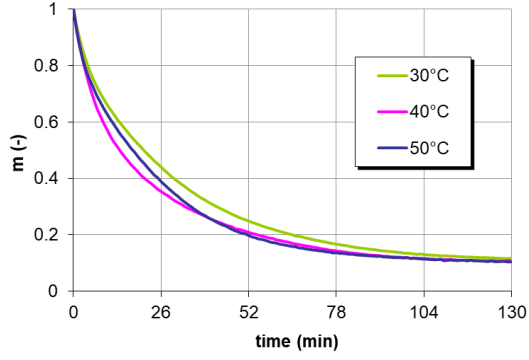


Figure 13: Drying curve of CA-THF at 0.2 m/s gas velocity

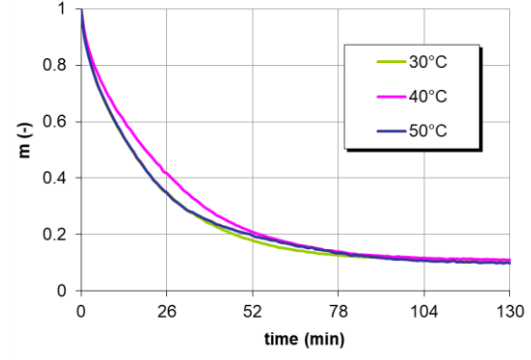


Figure 14: Drying curve of CA-THF at 0.5 m/s gas velocity

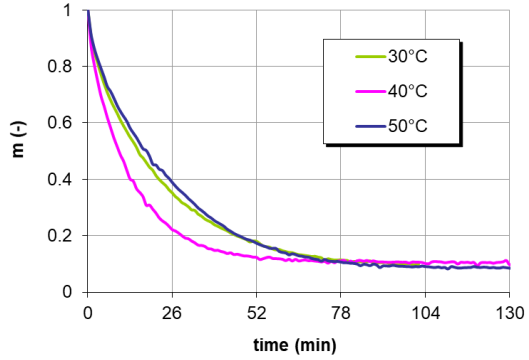


Figure 15: Drying curve of CA-THF at 0.8 m/s gas velocity

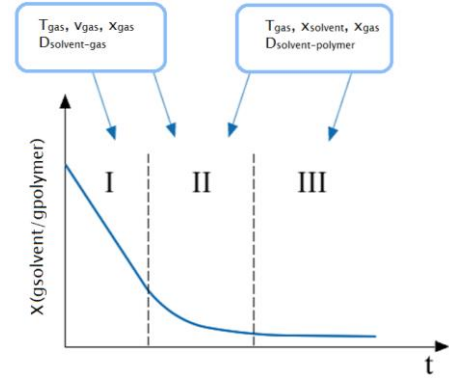


Figure 16: Drying curve of a polymer-solvent system

To model the drying of polymer films, the drying curve is divided into two periods, as follows: the first period, which is the first zone of drying, and the second period, which is composed of zone II and drying zone III.

At time  $t = 0$ , the film is brought into contact with hot air and the solvent starts to evaporate. Because the film support is made of a material that conducts heat very well (aluminum) and is kept in the dryer at constant temperature, heat transfer influence is neglected.

The following simplifying assumptions are considered:

- mass transfer is unidirectional, perpendicular to the thickness of the film;
- changing the size of the film takes place in the direction of its thickness;
- heat transfer outside is negligible;
- changing the size of the film is due only to solvent losses;
- solvent diffusion in the film follows Fick's first law; the direction of the diffusion is perpendicular to the film, the diffusion in the other directions is negligible;
- the tensions that appear in the film during drying are neglected.

With these specifications, the mass transfer to the drying of a polymeric film is described by the equations:

$$\frac{\partial \rho}{\partial t} = \frac{\partial}{\partial x} \left( D_A \frac{\partial \rho_A}{\partial x} \right) \quad (1)$$

$$\frac{\partial \delta}{\partial t} = \frac{\hat{v}_A \cdot D_A \left( \frac{\partial \rho_A}{\partial x} \right)}{1 - \rho_A \cdot \hat{v}_A} \quad (2)$$

where  $\rho_A$  – the volume concentration of the solvent;  $D_A$  – the diffusion coefficient of the solvent;  $\hat{v}_A$  – partial specific volume.

The initial conditions are as follows:

$$\rho_A = \rho_{A,0}; \quad t = 0$$

$$\delta = \delta_0; \quad t = 0 \quad 0 < x < \delta_0$$

The boundary conditions are:  $\frac{\partial \rho_A}{\partial t} = 0$ ;  $x = 0$

The solvent flow at the interface is described by the equation:

$$j_{A,s} = k_{g,A} (p_{A,i} - p_{A,0}) \quad (3)$$

where  $j_{A,s}$  is the solvent flux [Kg A/m<sup>2</sup>s]. This can be described as:

$$j_{A,s} = - \frac{d(\bar{\rho}_A \cdot \delta)}{dt} \quad (4)$$

where  $\bar{\rho}_A$  is the average value of the solvent volume concentration.

At equilibrium  $\rho_A = \rho_{A,eq}$  and  $x = \delta$ .

From the experimental data, drying period I has a duration of about 5 minutes for drying gas velocities  $v_{gas} > 0.4$  m/s and 7-8 minutes for  $v_{gas} < 0.4$  m/s. In this period,  $\bar{X}$  drops from 20 to 2-3 g<sub>solvent</sub>/g<sub>polymer</sub>.

Partial solvent pressure at the interface is determined with equilibrium pattern (Flory-Huggins), and for high solvent concentrations, activity can be considered  $a_{solvent} \approx 0.9-0.99$  and  $p_{sol}^{eq} \cong 0.95 \cdot p_{vap}^{(T)}$ .

$$N_A = k_g \cdot A \cdot (p_{vap}^{eq} - p_{vap}^{gas}) \quad (5)$$

The mass transfer coefficient  $k_g$  can be calculated using the following equations:

$$Sh_g = C \cdot Re_g^m \cdot Sc_g^n \quad (6)$$

$$Sh_g = \frac{k_g \cdot l}{D_{A,g}} \quad (7)$$

$$Re_g = \frac{v \cdot l \cdot \rho_g}{\eta_g} \quad (8)$$

$$Sc_g = \frac{\eta_g}{\rho_g \cdot D_{A,g}} \quad (9)$$

where  $Sh_g$  – Sherwood number;  $Re_g$  – Reynolds number;  $Sc_g$  – Schmidt number;  $l$  – characteristic length (the tunnel equivalent diameter was considered);  $v$  – gas velocity;  $\eta$  – gas viscosity;  $D_{A,g}$  – diffusion coefficient in gaseous phase.

For the evaporation of a solvent on a flat surface, the mass transfer is described by the relation:<sup>17</sup>

$$Sh_g = 0.664 \cdot Re_g^{0.5} \cdot Sc_g^{0.33} \quad (10)$$

During the second drying period, the transfer of the solvent into the polymer solution is controlled by diffusion and described by Fick's law. Considering that film dimensions, diffusion coefficient and temperature remain constant, the solution of the equation describing the variation of the solvent content over time is given by Crank:<sup>18</sup>

$$\bar{M} = \frac{M(t) - M_{eq}}{M_0 - M_{eq}} = \frac{8}{\pi^2} \sum_{n=0}^{\infty} \frac{1}{(2n+1)^2} \exp \left[ - \frac{(2n+1)^2 \pi^2 D_A t}{\delta^2} \right] \quad (11)$$

where:  $\bar{M}$  – normalized solvent mass;  $M_0$  – initial solution mass;  $M_{eq}$  – solution mass at equilibrium;  $M(t)$  – solution mass at time  $t$ ;  $\delta$  – film thickness [m];  $t$  – time [s];  $D_A$  – solvent-polymer diffusion coefficient [m<sup>2</sup>/s].

A similar form of Equation (11) for  $n = 3$  is given as follows:<sup>19</sup>

$$\frac{(w - w_e)}{(w_1 - w_e)} = \frac{8}{\pi^2} \left[ e^{-D_L t \left( \frac{\pi}{2l} \right)^2} + \frac{1}{9} e^{-9D_L t \left( \frac{\pi}{2l} \right)^2} + \frac{1}{25} e^{-25D_L t \left( \frac{\pi}{2l} \right)^2} + \dots \right] \quad (12)$$

where  $2l = \delta$ ;  $D_l = D_A$ ;  $w = M(t)$ ;  $w_e = M_{eq}$ ;  $w_1 = M_0$ .

Figure 17 shows the variation in the weight of the PVA-water film during drying. Both the experimental data and those calculated with Equations 5 (period I) and 12 (period II) are represented. From the figure, a good correlation is observed for a short time interval of the drying period I, in which the evaporation of the solvent from the solution can be considered as an evaporation of pure solvent on a surface. It is also observed that Equation 12 simulates well the variation of the normalized mass over the last time, in which the influence of the drying gas velocity is not pronounced. The solvent-polymer diffusion coefficient is maintained constant ( $D = 1.42E-12$ ) (determined on the basis of experimental diffusion data in the PVA-water system<sup>20</sup>). According to the model assumptions, the

dry film thickness is considered constant with a value of  $\delta = 120 \mu\text{m}$  only at long drying times. We considered a film thickness, which takes into account the solvent mass that decreases over time (variable thickness).

Since the analysis of the experimental data showed that the modification of the velocity of the drying gas has an insignificant influence on the mass variation over time, it was considered that the process is mainly influenced by the solvent-polymer diffusion. Thus, only Equation 12 was used for this system. For a more accurate simulation, the variation of the thickness of the film depending on the solvent concentration was considered in the model.

### Cellulose acetate-tetrahydrofuran

Diffusion data from the literature<sup>20</sup> was used to model the drying of CA-THF films. The coefficient of diffusion is influenced by temperature and concentration. At THF concentrations higher than 0.2 g/g<sub>CA</sub>, the value is approximately constant and independent of temperature. This value ( $D = 1.7 \text{ E-}11$ ) was considered for the simulations. Since the CA film has a porous structure, the thickness of the film was considered constant during the drying process.

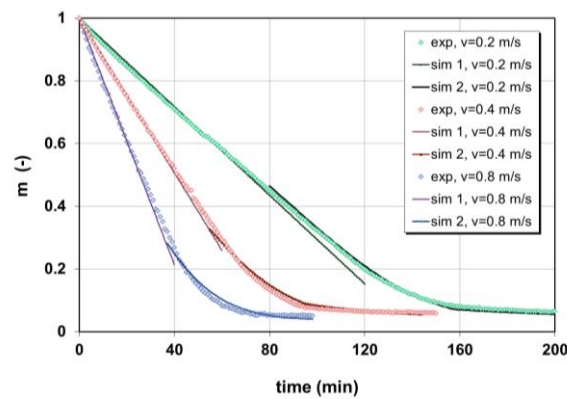


Figure 17: Comparison of experimental and simulated data for the PVA-water system – drying stages I and II at 50 °C

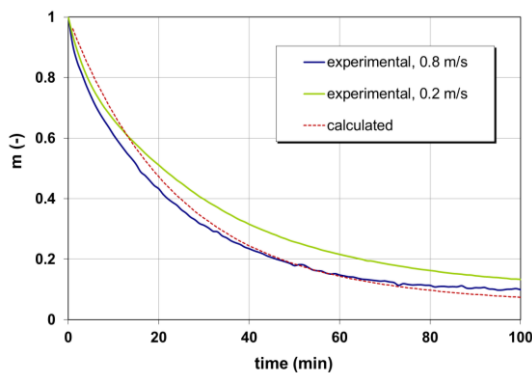


Figure 18: Comparison of experimental and simulated data for the CA-THF system at 30 °C

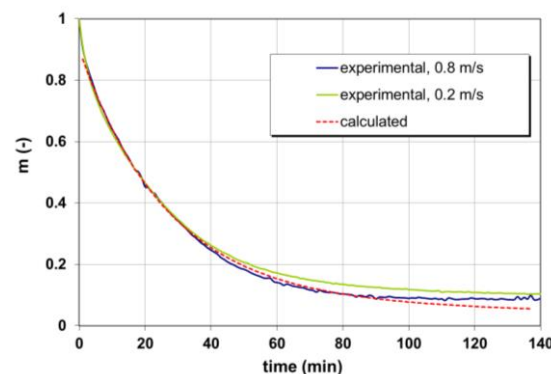


Figure 19: Comparison of experimental and simulated data for the CA-THF system at 50 °C

From the analysis of Figures 18 and 19, it can be observed that the results from the simulation have a satisfactory concordance with the experimental data. At low drying times, the deviation is up to 10% and at high values of time (over 40 min), it can exceed 50%. The model used does not take into account the first drying period, which is characteristic only of the removal of solvent from compact polymers.

### CONCLUSION

Drying of polymer films and membranes is a complex process influenced by many interacting factors. The main objective of the research reported in this paper was the study of the influence of the



main factors contributing to the drying of polymer films. In the experiments, two polymer-solvent systems (PVA-W and CA-THF) have been used, which have different drying behavior.

The influence of gas velocity and temperature on the drying behavior of the films was emphasized using a set-up designed in our laboratory. Polymer drying is influenced by both temperature and gas velocity, but also by the appearance of a skin at the liquid-gas interface (possibly for PVA-W at temperatures higher than 50 °C and for CA-THF, at temperatures higher than 40 °C). If this occurs, this skin limits the mass transfer from the liquid to the gaseous phase as a result of the pronounced decrease of the diffusion coefficient.

Generally, when removing solvents from polymeric solutions, three areas can be highlighted on the drying curves, as evidenced in the experimental studies on PVA-water. For the CA-THF system, these areas cannot be clearly marked.

Polymer-solvent binary systems have a complex drying behavior and a minimal adjustment of the parameters can make a difference between a film that can qualitatively meet technical requirements and one that cannot be used.

Numerical calculations are a helpful completion of experimental investigations. They can help reduce the number of experiments and thus save resources. On the other hand, experimental data are necessary for the simulation.

## REFERENCES

- <sup>1</sup> A. J. M. Valente, A. Y. Polishchuk, H. D. Burrows and V. M. M. Lobo, *Eur. Polym. J.*, **41**, 275 (2005), <https://doi.org/10.1016/j.eurpolymj.2004.09.022>
- <sup>2</sup> W. Schabel, P. Scharfer, M. Kind and I. Mamaliga, *Chem. Eng. Sci.*, **62**, 2254 (2007), <https://doi.org/10.1016/j.ces.2016.12.062>
- <sup>3</sup> B. Guerrier, C. Bouchard, C. Allah and C. Benard, *AIChE J.*, **44**, 791 (1998), <https://doi.org/10.1002/aic.690440404>
- <sup>4</sup> Y. Huang, H. Liu and Y. Hu, *Chem. Eng. Sci.*, **59**, 3649 (2004), <https://doi.org/10.1016/j.ces.2004.05.026>
- <sup>5</sup> M. Han, B. Zhao, X. M. Zhang and W. J. Zhang, *Chem. Eng. Proc.*, **47**, 245 (2008), <https://doi.org/10.1016/j.cep.2007.01.032>
- <sup>6</sup> H. Hezaveh and I. I. Muhamad, *Chem. Eng. Res. Des.*, **91**, 508 (2013), <https://doi.org/10.1016/j.cherd.2012.08.014>
- <sup>7</sup> S. Gustaite, J. Kazlauskas, J. Bobokalonov, S. Perni, V. Dutschk *et al.*, *Colloid. Surfaces A*, **480**, 336 (2015), <https://doi.org/10.1016/j.colsurfa.2014.08.022>
- <sup>8</sup> N. A. Abdelwahab, N. S. Ammar and H. S. Ibrahim, *Int. J. Biol. Macromol.*, **79**, 913 (2015), <https://doi.org/10.1016/j.ijbiomac.2015.05.022>
- <sup>9</sup> Z. Zhang, Y. Cao, L. Chen and Z. Huang, *Cellulose Chem. Technol.*, **51**, 559 (2017), [http://www.cellulosechemtechnol.ro/pdf/CCT5-6\(2017\)/p.559-567.pdf](http://www.cellulosechemtechnol.ro/pdf/CCT5-6(2017)/p.559-567.pdf)
- <sup>10</sup> S. Um-I-Zahra, H. Li and L. Zhu, *Cellulose Chem. Technol.*, **51**, 899 (2017), [http://www.cellulosechemtechnol.ro/pdf/CCT9-10\(2017\)/p.899-909.pdf](http://www.cellulosechemtechnol.ro/pdf/CCT9-10(2017)/p.899-909.pdf)
- <sup>11</sup> R. G. Candido, G. G. Godoy and A. R. Gonçalves, *Carbohydr. Polym.*, **167**, 280 (2017), <https://doi.org/10.1016/j.carbpol.2017.03.057>
- <sup>12</sup> D. Thomas, E. Zuravlev, A. Wurm, C. Schick and P. Cebe, *Polymer*, **137**, 145 (2018), <https://doi.org/10.1016/j.polymer.2018.01.004>
- <sup>13</sup> T. S. Gaaz, A. B. Sulong, M. N. Akhtar, A. H. Khadhum, A. B. Mohamad *et al.*, *Molecules*, **20**, 22833 (2015), <https://doi.org/10.3390/molecules201219884>
- <sup>14</sup> S. Fischer, K. Thümmel, B. Volkert, K. Hettrich, I. Schmidt *et al.*, *Macromol. Symp.*, **262**, 89 (2008), <https://doi.org/10.1002/masy.200850210>
- <sup>15</sup> R. G. Candido and A. R. Gonçalves, *Carbohydr. Polym.*, **152**, 679 (2016), <https://doi.org/10.1016/j.carbpol.2016.07.071>
- <sup>16</sup> O. A. Deorukhkar, B. S. Deogharkar and Y. S. Mahajan, *Chem. Eng. Process.*, **105**, 76 (2016), <https://doi.org/10.1016/j.cep.2016.04.006>
- <sup>17</sup> “VDI-Waermeatlas”, 8<sup>th</sup> edition, Springer-Verlag, Berlin, 1997, pp. A 43-A 44, ISBN 3-540-62719-8, <https://www.springer.com/de/>
- <sup>18</sup> J. Crank, “The Mathematics of Diffusion”, 2<sup>nd</sup> edition, Clarendon Press, Oxford, 1975, ISBN 0198533446, <http://clarendonpress.com/>
- <sup>19</sup> J. F. Richardson, J. H. Barker and J. R. Backhurst, “Coulson and Richardson’s Chemical Engineering”, vol. 2, 5<sup>th</sup> edition, Butterworth-Heinemann, Oxford, 2002, pp. 912, ISBN 0750644451, <https://www.elsevier.com/books-and-journals/butterworth-heinemann>
- <sup>20</sup> C. C. Negoescu, Doctoral thesis, Technical University of Iasi, 2013